Tuijin Jishu/Journal of Propulsion Technology
ISSN: 1001-4055
Vol. 44 No. 5 (2023)

Effect of Zinc Nitrate on Morphology and Particle Size of Nano-sized Zinc Oxide

V. S. Kalyamwar[1]*, S. D. Charpe[2], S. S. Kawar[3], R. B. Pedhekar[4] P.D. Shirbhate[5]

[1] Department of Physics, Bharatiya Mahavidyalaya, Amravati, India*

[2]Department of Physics, J. D. Patil Sangludkar Mahavidyalaya, Daryapur Dist. Amravati, India

[3] Department of Physics, Dr. R. G. Rathod Arts & Science College, Murtizapur Dist. Akola, India

[4]Mahatma Jyotiba Fule Commerce, Science & Vitthalrao Raut Arts College, Bhatkuli, Dist. Amravati, India.

[5] Department of Physics, Gopikabai Sitaram Gawande Mahavidyalaya, Umarkhed Dist. Yavatmal, India.

Abstract:

Zinc oxide nanostructures were synthesized by chemical route method. The XRD spectrum indicates that the sample is wurtezite (hexagonal) structured ZnO with lattice constants of a = 3.249A0, c = 5.206 A0. The crystallinity and structure of these ZnO nanostructures were studied by X-ray diffraction. The morphologies of these synthesized nanostructures were analyzed by transmission electron microscope. Effects of concentration of zinc nitrate during synthesis on the morphology and particle size of resultant product were investigated.

***Keywords**: Chemical route method, Zinc oxide*

Introduction

Semiconductor nanostructures are a very important topic in the ongoing research activity across the world. As the semiconductor particles exhibit size dependent properties like scaling of the energy gas and corresponding change in the optical properties, they are considered as the front runners in the technologically important materials.

Zinc oxide is attracting tremendous attention due to its interesting properties like wide direct band gap of 3.37 eV at room temperatures and high exciton binding energy of 60 meV. Zinc oxide is promising materials for electronics or optoelectronics applications such as solar cells, gas sensors, liquid crystal displays, heat mirrors, surface acoustics wave devices etc [1-10].

A variety of techniques like spray pyrolysis, molecular beam epitaxy, chemical vapor deposition, hydrothermal method, pulsed laser deposition, sol-gel method, laser ablation [11-17] etc. have been widely used to synthesis ZnO nanostructures.

In the present study, ZnO nanostructures were synthesized by using chemical route method. The crystallinity and structure of these ZnO nanostructures were studied by X-ray diffraction. The morphologies of these synthesized nanostructures were analyzed by transmission electron microscope.

Experimental

All chemicals were of analytical grade and were used as purchased without further purification.

In typical process, 2.974 g $Zn(NO_3)_2 \cdot 6H_2O$ (Zinc nitrate hexahydrate) was dissolved in 100ml distilled water and 2.0 g of NaOH was dissolved in 100 ml distilled water. The zinc nitrate solution was added drop wise to the NaOH solution to form white solution. Then, white solution was subsequently kept at 75^0C For 12 hr. The resulting white precipitates were collected, washed with distilled water and ethanol several times and then dried at 80^0C in vacuum oven for 2hr. Resultant product was treated as 0.1 M ZnO since during process 0.1M zinc nitrate solution was used.

Similar procedure were adopted to synthesized 0.05M ZnO, 0.15M ZnO and 0.2M ZnO by keeping concentration of zinc nitrate 0.05M, 0.15M and 0.2M respectively.

Results and discussion

1. X-ray diffraction

X-ray diffraction data for structural characterization of various products synthesized by chemical route method were collected on the Philips PW 1710 X-ray Diffractometer using Cu-Kα source. X-ray diffraction pattern of various synthesized products are helpful in studying the crystalline structure and determination of crystallite size.

Figure 1(a) to 1(d) shows XRD pattern of 0.05M ZnO, 0.1M ZnO, 0.15M ZnO and 0.2M ZnO respectively. The recorded XRD pattern of 0.05M ZnO confirmed that synthesized ZnO are highly crystalline in nature.

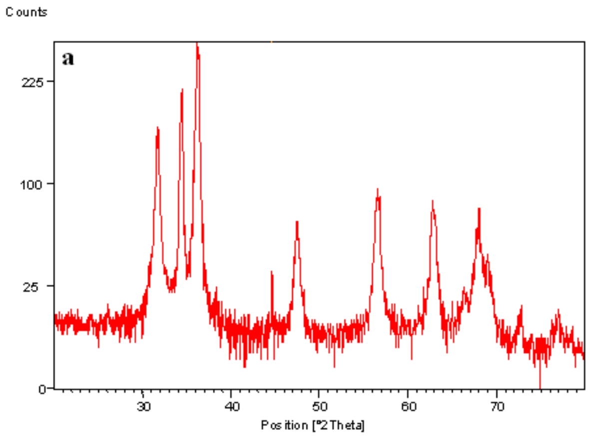

Figure 1(a) powder XRD pattern of 0.05M ZnO

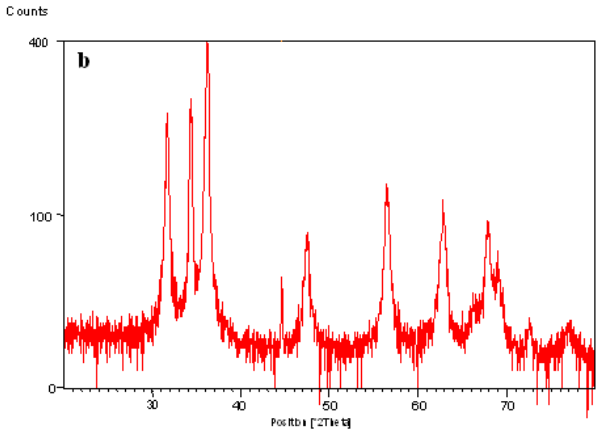

Figure 1(b) powder XRD pattern of 0.1M ZnO

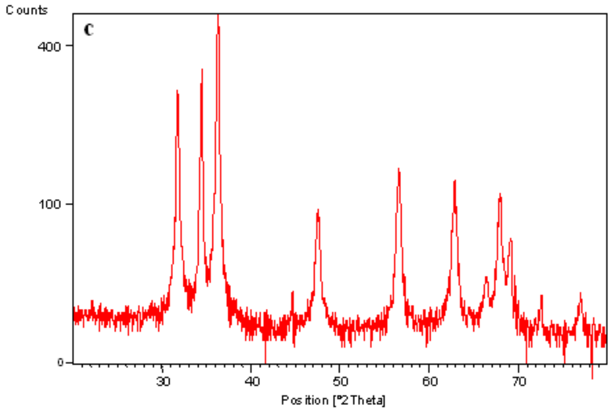

Figure 1(c) powder XRD pattern of 0.15M ZnO

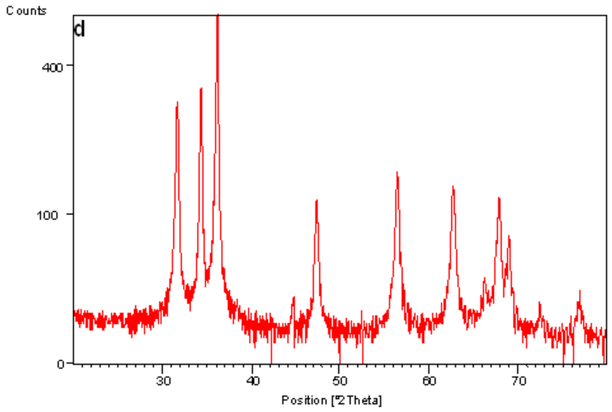

Figure 1(d) powder XRD pattern of 0.2M ZnO

The corresponding X-ray diffraction peak for (100), (002), (101) and (102) planes confirm the formation of hexagonal wurtzite structure of ZnO, which are in good agreement with the literature values (JCPDS card No. 36-1451). In this XRD pattern, extra pick appear at $2\theta = 44^0$. This peak was identified as surface hydroxyl groups, which can be related to the formation of water on the ZnO nanostructure surface [18]. Also XRD pattern of the 0.1M ZnO, 0.15M ZnO and 0.2M ZnO shows parallel results.

The table 1 shows the comparison of obtained XRD data with standard data (JCPDS card No. 36-1451).

Sample	Observed		Standard (JCPDS card No. 36-1451)		(h k l) Plane
	2θ	'd' Values (A^0)	2θ	'd' Values (A^0)	
0.05M ZnO	31.7008	2.82030	31.770	2.8143	(1 0 0)
	34.4878	2.59850	34.422	2.6033	(0 0 2)
	36.3819	2.46754	36.253	2.4759	(1 0 1)
0.1M ZnO	31.6854	2.8263	31.770	2.8143	(1 0 0)
	34.3774	2.60659	34.422	2.6033	(0 0 2)

	36.2095	2.47880	36.253	2.4759	(1 0 1)
0.15M ZnO	31.7805	2.8134	31.770	2.8143	(1 0 0)
	34.4793	2.59912	34.422	2.6033	(0 0 2)
	36.3109	2.47210	36.253	2.4759	(1 0 1)
0.2M ZnO	31.7036	2.82006	31.770	2.8143	(1 0 0)
	34.3174	2.61101	34.422	2.6033	(0 0 2)
	36.1648	2.48176	36.253	2.4759	(1 0 1)

To extract more information on the crystallinity, the XRD data is exercised to determine the crystallite size. The full width at half maxima (FEHM) of the intense (101) peak was evaluated for all the ZnO nanostructures, by using Scherrer's formula [19, 20].

$D = k\lambda/\beta\sin\theta$

Where λ is the wavelength of incident beam (1.5406 A^0), β is the FWHM of the peak in radians, θ is the diffraction angle and k is Scherrer constant.

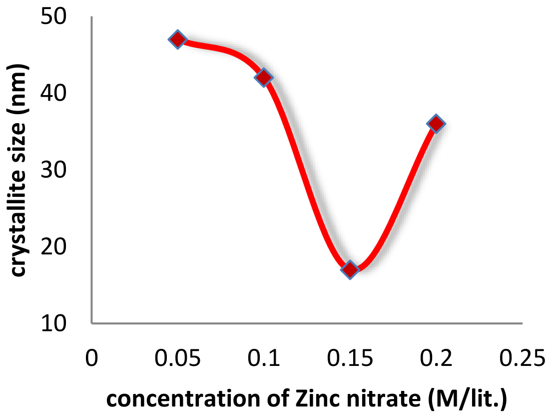

Figure 2 variation of crystallite size with concentration of zinc nitrate

Figure 2 shows the variation of crystallite size of synthesized ZnO with the concentration of Zinc nitrate during synthesis.

The influence of the concentration of zinc nitrate on the particle size of product was the main subject of interest here. Figure 2 shows the variation of crystallite size of synthesized ZnO with its reactant concentration. It is seen that crystallite size decreases with concentration of zinc nitrate, conquer minimum value (17 nm) at 0.15M Concentration and for further higher concentration of zinc nitrate it increases. The increase in crystallite size with increasing concentration of zinc nitrate may be due to accumulation of ZnO nanoparticles to form crystallite of higher size.

Transmission electron microscope

The morphology and particle size of ZnO samples synthesized by chemical route method were examined by using Techai G2 20 Ultra-Twin transmission electron microscope (Pune University, Pune). For the TEM observation, the as-prepared samples were added into an alcohol solution and subjected to violent ultrasonic stirring for hours; subsequently, a drop of this solution was dipped on a copper grid used for the TEM observation.

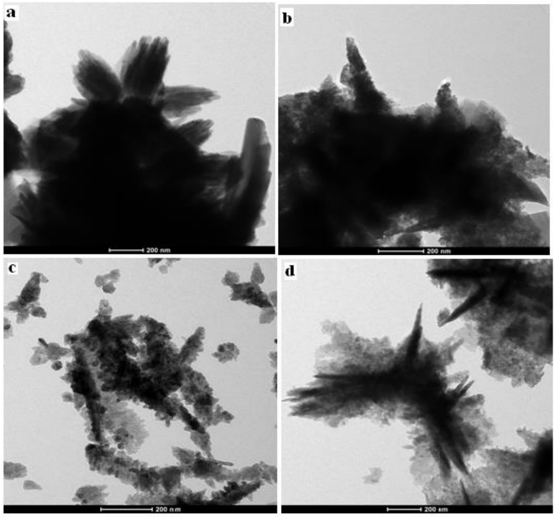

Figure 3 TEM images of a) 0.05M ZnO, b) 0.1M ZnO, c) 0.15M ZnO, d) 0.2M ZnO

Figure 3 represent TEM images of the products obtained by chemical route method with different concentration of Zinc nitrate. Figure 3(a) shows the formation of nanoparticles featuring the occurrence of surrounding pyramids by using 0.05N zinc nitrate during synthesis. The formation of pyramid can be ascribed to the anisotropic growth of ZnO crystal. As the concentration of reactant increased to 0.1M, the nanoparticles of ZnO further coarsened (figure 3b). Further, increases in concentration of zinc nitrate to 0.15M, most of the pyramids get separated from the branched nanocrystals; formation of nanorods and nanoparticles takes places with average particle size of 15 to 25 nm. Figure 3(d) represent that further increasing the zinc nitrate concentration to 0.2M, formation of branched nanocrystals were observed.

Zinc oxide nanostructure growth mechanism

In chemical route method when zinc nitrate reacts with sodium hydroxide formation of $Zn(OH)_2$ along with $Zn(OH)_4^{2-}$ takes place. The concentration of $Zn(OH)_4^{2-}$ are kept constant in the reaction process because $Zn(OH)_2$ is dissolved by the OH^- produced by the decomposition of $Zn(OH)_4^{2-}$ according to following reactions,

$$Zn(OH)_2 + 2OH^- \rightarrow Zn(OH)_4^{2-}$$

$$Zn(OH)_4^{2-} \rightarrow ZnO + H_2O + 2OH^-$$

The stable concentration of $Zn(OH)_4^{2-}$ may be important for controlling the growth rate of different crystal faces of ZnO.

Form the results of XRD it is clear that ZnO synthesized by chemical route method keeping 0.15M concentration of zinc nitrate yield the products with small crystallite size. Such products with small crystallite size and innovative morphology can be used as sensor elements.

Conclusion

From the results obtained, following statements can be made for the synthesized ZnO nanostructures by hydrothermal and chemical route method.

1. Zinc Oxide nanostructures synthesized by chemical route method show highly crystalline in nature with hexagonal wurtzite structure.
2. When the concentration of zinc nitrate was kept 0.15M during reaction in chemical route method, resultant ZnO nanostructure produce with a lowest crystallite size 17nm among other products.

References:

[1] Chopra L., Major S., Panday D. K., Thin Solid Films, **1021,** (1983) pp. 1-4.

---

[2] Bose S., Barua A. K., Journal of Physics D: Applied Physics, **32,** (1999) pp. 213-218. doi: 10.1088/0022-3727/32/3/006

[3] Kim H., Gilmore C. M., Applied Physics Letters, **76**, (2000) pp. 259-261. https://doi.org/10.1063/1.125740

[4] Xia Y., Hu C. G., Han X. Y., Xiong Y. F., Gao P. X., Liu G. B., Solid State Communications, **141,** (2007) pp. 506–509. https://doi.org/10.1016/j.ssc.2006.12.016

[5] Ki Won Kim, Pyeong Seok Cho, Sun Jung Kim, Jong Heun Lee, Chong Yun Kang, Jin Sang Kim, Seok Jin Yoon, Sensors and Actuators B, **123,** (2007) pp. 318–324. https://doi.org/10.1016/j.snb.2006.08.028

[6] Forleo A., Francioso L., Capone S., Siciliano P., Lommens P., Hens Z., Sensors and Actuators B, **146,** (2010) pp. 111–115. https://doi.org/10.1016/j.snb.2010.02.059

[7] Badadhe Satish S., Mulla I.S., Sensors and Actuators B, **143,** (2009) pp. 164–170. https://doi.org/10.1016/j.snb.2009.08.056

[8] Lupan O.I., Shishiyanu S.T., Shishiyanu T.S., Superlattices and Microstructures, **42,** (2007) pp. 375–378. https://doi.org/10.1016/j.spmi.2007.04.009

[9] Sarala Devi G., Bala Subrahmanyam V., Gadkari S.C., Gupta S.K., Analytica Chimica Acta, **568,** (2006) pp. 41–46. https://doi.org/10.1016/j.aca.2006.02.040

[10] Ravi Chand Singh, Onkar Singh, Manmeet Pal Singh, Paramdeep Singh Chandi, Sensors and Actuators B, **135,** (2008) pp. 352–357. https://doi.org/10.1016/j.snb.2008.09.004

[11] Shinde V. R., Lokhande C. D., Mane R. S., Han S. H., Applied Surface Science, **245,** (2005) pp. 407-413. https://doi.org/10.1016/j.apsusc.2004.10.036

[12] Morgan J. H., Broide D. E., Canadian Journal of Physics, **60,** (1982) pp. 1387-1390. https://doi.org/10.1139/p82-186

[13] Craciun V., Elders J., Gardeniers J. G. E., Geretovsky J., Boyd I. W., Thin Solid Films, **259,** (1995) pp. 1-4.

[14] Ohyama M., Kozuka H., Yoko T., Thin Solid Films, **306,** (1997) pp. 78-85. https://doi.org/10.1016/S0040-6090(97)00231-9

[15] Ayouchi R., Leinen D., Martin F., Gabas M., Dalchiele E., Ramos Barrado J. R., Thin Solid Films, **426,** (2003) pp. 68-77. https://doi.org/10.1016/S0040-6090(02)01331-7

[16] Paraguay F., Morales J., Estrada W., Andrade E., Yoshida M. M., Thin Solid Films, **366,** (2000) pp. 16-27. https://doi.org/10.1016/S0040-6090(00)00752-5

[17] Moustaghfir A., Tomasella E., Amor S. B., Jacquet M., Cellier J., Sauvage T., Surface and Coating Technology, **193,** (2003) pp. 174-175. https://doi.org/10.1016/S0257-8972(03)00417-1

[18] Kester W J Wong, Matthew R Field, Jian Zhen Ou, Kay Latham, Michelle J S Spencer, Irene Yarovsky, Kourosh Kalantar-zadeh, *Nanotechnology*, **23,** (2012) pp. 015705-015713

[19] Hilber T., Letonja P., Marr R., Poit P., Siebenhofer M. Part. Part. Syst. Charact., **19,** (2002) pp. 342-347. **https://doi.org/10.1002/1521-4117(200211)19:5<342::AID-PPSC342>3.0.CO;2-6**

[20] Charpe, S. D., Raghuwanshi, F. C., Lamdhade, G. T., & Kalyamwar, V. S., Journal of Electrical Engineering, **3,** (2015) pp. 12-17.